Table 1A Results of analysis of the chromosome region that shows amplification by CGH.

chromosome	PC-1	PC-3	PC-7	PC-10	PC-14
1	1q31-q32 1q41-q44	1p12-p11 1q11-q12	1p22-p21 1q21-q25 1q31-q32	1q43-q44	1q12
2		2p15-p11 2q11-q14 2q21-q24		2p21 2q12-q13 2q22-q23	2p22 2q24
3	3p11		3q21-q24	3p26 3q12-q12 3q24-q28	3p11 3q11 3q24 3q27
4	4p12 4q11-q13	4q12	4p16-p15 4q12-q13		
5	5q11-q13			5p15-p11	5p25-p21 5q31-q35
6		6p25-p21 6q25-27	6p25-p22 6p12		6p25-p21 6p12-p11
7	7p22	7q21-q22 7q31-q32	7p15-p13 7q21-q22 7q31-q36	7p22-p21 7p15-p11 7q11 7q21-q22	7p22
8	8p23 8q11-q13 8q21	8p23-p21 8p12-p11	8p12-p11 8q21-q24		8q11-q13 8q21-q24
9			9q34		9q34
10					
11	11q13-q14 11q23 11q25			11p15	11p15 11q13 11q25
12		12p13-p11	12p12 12q21		12p13
13			13q31-q34		13q14 13q21 13q34
14					14q11-q13 14q21-24 14q32
15			15p15		
16		16q11 16q13 16q21-q22			16q21-q24 16q11-q13
17					
18		18p11 18q11-q12			18q11
19					
20		20p13	20p13-p11	20p12	20p11
21					
22					22q13-q11
X	Xp22 Xq11-q12 Xq22 Xq26				Xp11 Xq11
Y					

Table 1B Results of analysis of the chromosome region that shows loss by CGH.

chromosome	PC-1	PC-3	PC-7	PC-10	PC-14
1	1p36			1p31 1p22-p21 1p12-p11 1q11 1q21	
2	2p25		2q31		2q12 2q37
3			3p21 3q29		
4			4q28 4q34-q35	4p16-p15 4q31 4q35	4p16 4q24-q26
5			5p15	5q12 5q21-q23 5q35	
6	6q27		6q25-q27		6q13 6q25-q27
7					7p15 7q36
8		8q12-q13 8q21		8p23-p21 8p12-p11	
9	9q12	9p13 9p11 9q11-q13 9q21-q22 9q32		9p23 9p11 9q11-q13 9q21 9q34	9p21
10		10p11	10p11	10p15-p13 10p11 10q11	10p15 10q21-q22 10q24 10q26
11	11p15	11p11	11q22-q24	11p11 11q11-q12	
12		12q24			12q24
13	13p11 13q21-q22	13p13-p11 13q11-q12 13q21 13q31-q34	13p13-p11 13q11-q13	13q22-q23 13q33-q34	13p13-p11
14	14p13 14p11	14p13-p11 14q31	14p13-p11	14p13-p11 14q11	14p12
15		15p13-p11 15q11	15p12-p11	15q11	15p12-p11 15q11 15q24 15q26
16			16q11	16q11-q12	16p13
17	17p13	17p13-p11	17p13-p11		
18	18p11	18q22-q23	18q11-q12 18q21		18p11 18q22-q23
19	19q13	19p13-p11		19p13	
20					
21		21p13-p11	21p13-p11 21q20		21p13-p11 21q21
22	22p13-12	22p13-p11	22p12-p11 22q11 22q13		22p12
X		Xp22		Xp22 Xp11	Xp22
Y	Yp11 Yq11-q12	Yp11 Yq11-q12		Yp11	Yp11 Yq11-q12

の細胞株細胞株に共通してみられた領域は4q35、6q27、10p11、11p11、12q24、13p11、13q14、17p13などであった。

2. Genomic DNA microarray法による解析結果

人の癌で増幅が報告されている59遺伝子に焦点をあてて解析した (Table 2)。

緑色と赤色の蛍光強度の比が1.5以上を増幅と判定し、グラフに示した (Fig. 2A-E)。PC-1ではMYCN(2p24.1)、RAF1(3p25)、MYB(6q22)、ESR(6q25.1)、FGFR1(8p11.2-p11.1)、PAK1(11q13.5-q14)、CCND2(12p13)、JUNB(19p13.2)、BCR(22q11.21)の癌遺伝子が増幅を示した。PC-3ではPAK1が増幅を示した。PC-7ではPDGFRA(4q12)、PGY1(7q21.1)、MET(7q31)が増幅を示した。PC-10ではEGFR(7p12.3-p12.1)、PGY1(7q21.1)、H-ras(11p15.5)、ERBB2(17q21.2)が増幅を示した。PC-14ではfluorescence ratio1.5≦rの増幅は認めなかった。

3. CGH法とgenomic DNA microarray法の結果の比較

CGH法とgenomic DNA microarray法の二法で解析し一致した増幅遺伝子の染色体領域について、相関図で示した (Fig. 3A-3C)。PC-3においてはそれぞれの方法で増幅領域は解析されたが、二法で合致する領域は検出出来なかった。PC-14では、genomic DNA microarray法では増幅を認めなかった。

考　察

今回CGH法とgenomic DNA microarray法の二法により肺癌細胞株の遺伝子増幅について解析を行った。

Table 2 DNA probes used for genomic DNA microarray analysis.

	gene	location		gene	location
1	FGR	1p36.2-p36.1	31	WNT1	12q12-q13
2	MYCL1	1p34.3	32	GLI	12q13.2-q13.3
3	N-ras	1p13.2	33	SAS/CDK	12q13.3
4	LAMC2	1q25-q31	34	MDM2	12q14.3-q15
5	MYCN	2p24.1	35	AKT1	14q32.3
6	REL	2p13-p12	36	IGFR1	15q25-q26
7	RAF1	3p25	37	FES	15q26.1
8	TERC	3q26.3	38	MRP1	16p13.1
9	PIK3CA	3q26.3	39	TOP2A	17q21-q22
10	PDGFRA	4q12	40	ERBB2	17q21.2
11	MYB	6q22	41	RPS6KB1	17q23
12	ESR	6q25.1	42	D17S167	17q23
13	EGFR	7p12.3-p12.1	43	YES1	18p11.3
14	PGY1	7q21.1	44	BCL2 3′	18q21.3
15	MET	7q31	45	BCL2 5′	18q21.3
16	CTSB	8p22	46	INSR	19p13.2
17	FGFR1	8p11.2-p11.1	47	JUNB	19p13.2
18	MOS	8q11	48	CCNE1	19q13.1
19	MYC	8q24.12-q24.13	49	AIB1	20q12
20	ABL1	9q34.1	50	STK15	20q13
21	FGFR2	10q26	51	CSE1L	20q13
22	H-ras	11p15.5	52	MYBL2	20q13.1
23	CCND1	11q13	53	PTPN1	20q13.1-q13.2
24	FGF4/FG	11q13	54	ZNF217	20q13.2
25	EMS1	11q13	55	CBFA2	21q22.3
26	GARP	11q13.5-q14	56	BCR	22q11.21
27	PAK1	11q13.5-q14	57	PDGFB	22q12.3-q13.1
28	MLL	11q23	58	AR 5′	Xq11-q12
29	CCND2	12p13	59	AR 3′	Xq11-q12

59 genes previously reported to be amplified in human cancer.

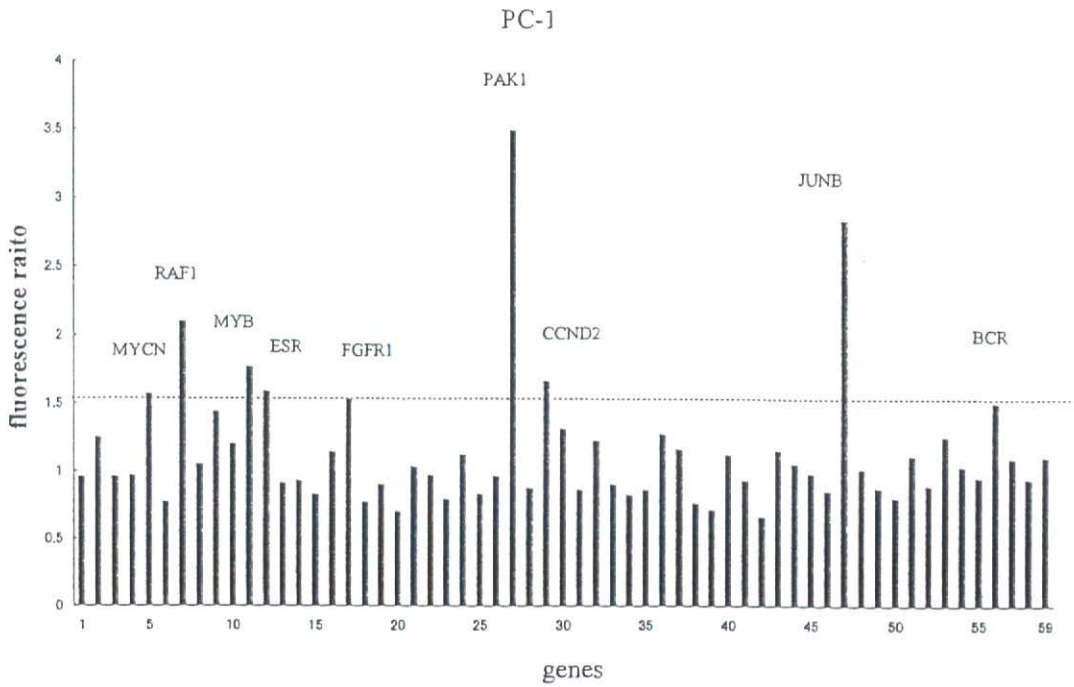

Fig. 2A Results of analysis of PC-1 by genomic DNA microarray. Amplifications in MYCN, RAF1, MYB, ESR, FGFR1, PAK1, CCND2, JUNB, BCR were observed.

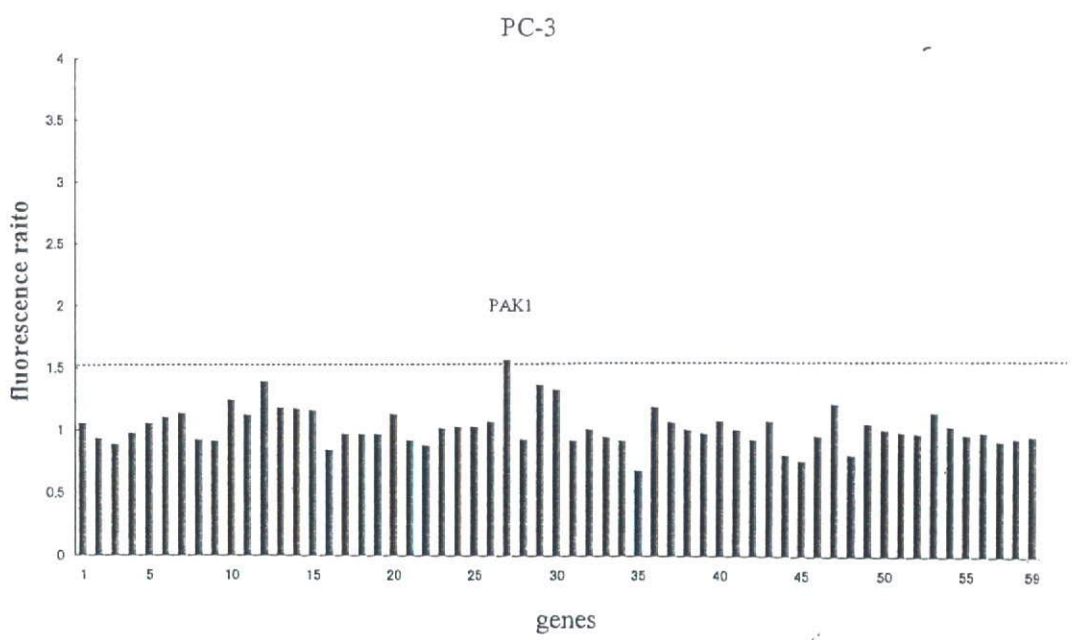

Fig. 2B Results of analysis of PC-3 by genomic DNA microarray. Amplification in PAK1 was observed.

CGH 法は一度に染色体全領域のコピー数異常が検出できる簡便な方法であるが、染色体上の遺伝子異常をピンポイントで捕らえることは出来ない。CGH 法での解析で問題となるのは、検出感度が遺伝子異常の領域の長さとその程度に依存することである。遺伝子異常では増幅が検出されやすい。増幅単位が 5 Mb 以上であれば、2 倍の増幅レベルからでも検出可能である。増幅単位が 300 Kb という短い領域での増幅を検出する場合は 5〜10 倍以上の増幅レベルで検出可能となる。一方、欠失領域の検出感度は低く、5 Mb 以上の欠失がないと遺伝子欠失は検出されにくい。増幅、欠失領域ともに 20 Mb 以下の場合、検出感度は十分で

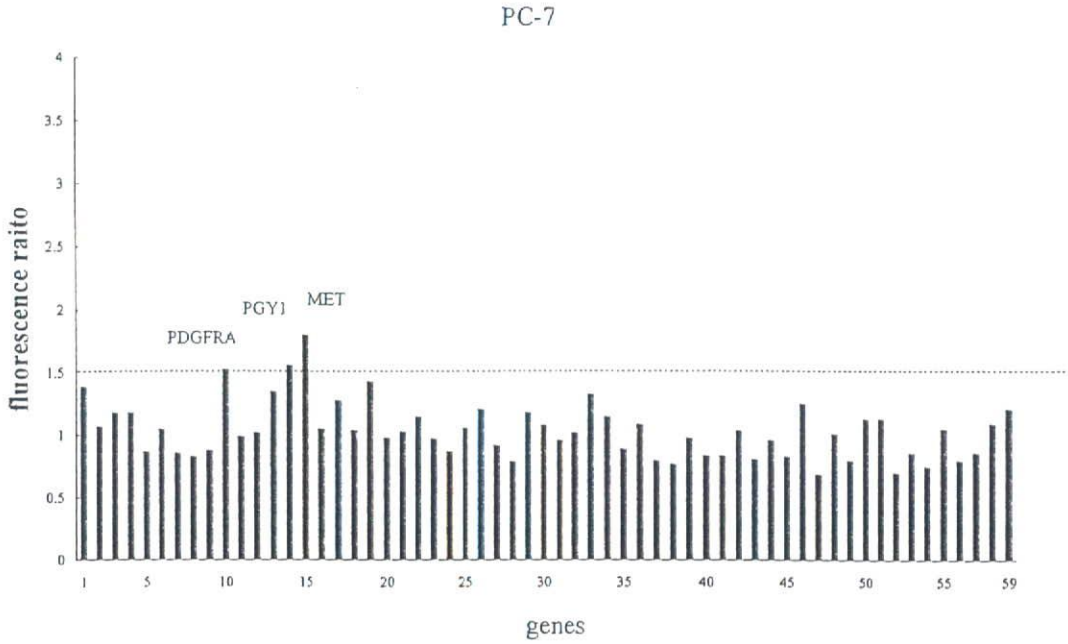

Fig. 2C　In PC-7 amplifications in PDGFR, PGY1, and MET were observed.

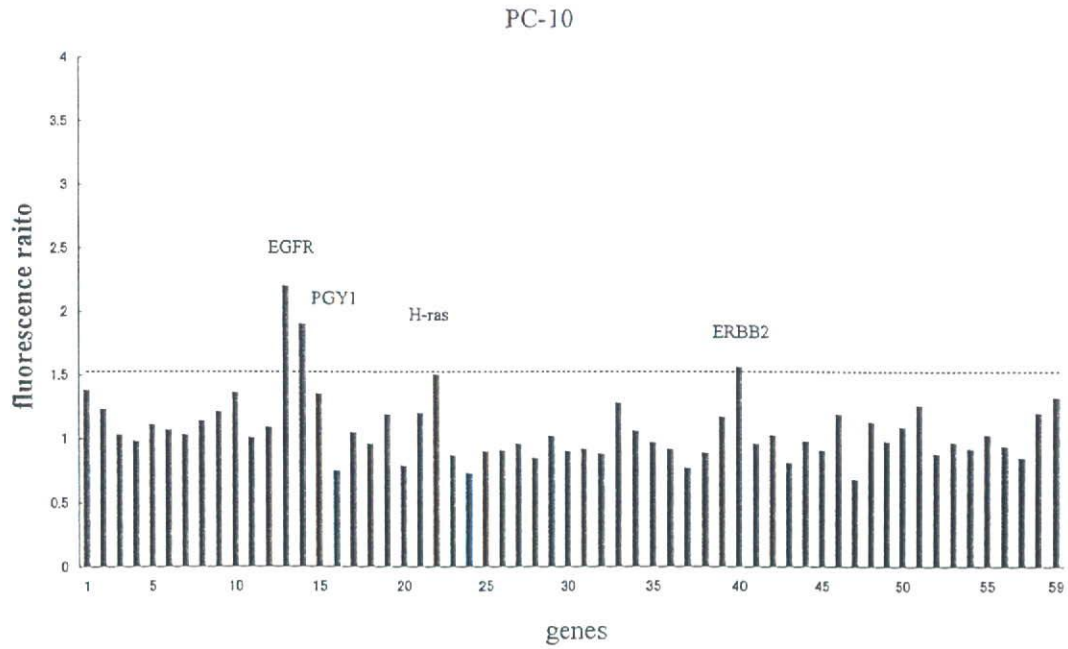

Fig. 2D　Genomic DNA microarray analysis showed amplifications of EGFR, PGY1, H-ras, ERBB2 in PC-10.

ない[17]。また、検体の癌細胞に正常細胞が混在していると検出感度は低下する。50%以上の正常細胞の混入は、解析の意味をなさないとされる。

一方 genomic DNA microarray 法は遺伝子個々のコピー数について解析できるが、当然アレー上にない未知の遺伝子についての情報は得られない。従って両者は、それぞれ目的に応じて使いわけられている。

今回の実験では5種類の肺癌細胞株を CGH 法と genomic DNA microarray 法の二法で比較解析を行ったが増幅を示す染色体異常領域に含まれる遺伝子異常は全てが一致というわけにはいかなかった。この結果は、それぞれの解析法の長所、短所に起因するのかもしれない。前述したように、CGH 法では染色体上で DNA コピー数の変化を巨視的にみるので、増幅にしても欠失にしてもかなり長い距離の変化をみていることになると考えられる。Genomic DNA microarray

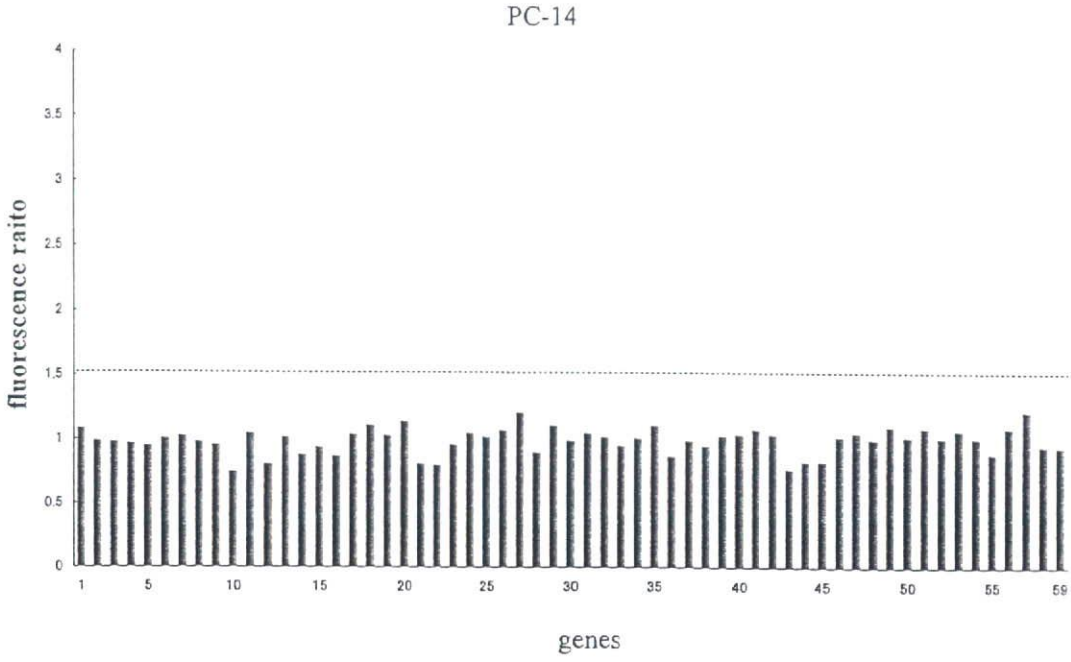

Fig. 2E　Genomic DNA microarray analysis did not show amplifications in PC-14.

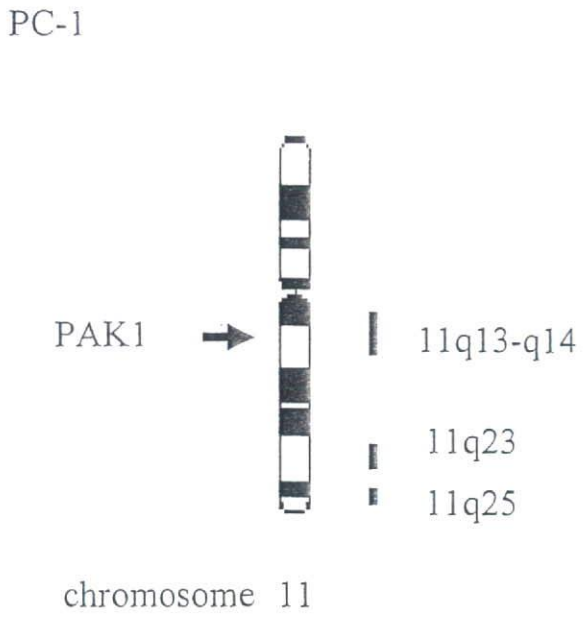

Fig. 3A　Gene and chromosome regions that showed amplification by CGH analysis and genomic DNA microarray in PC-1.

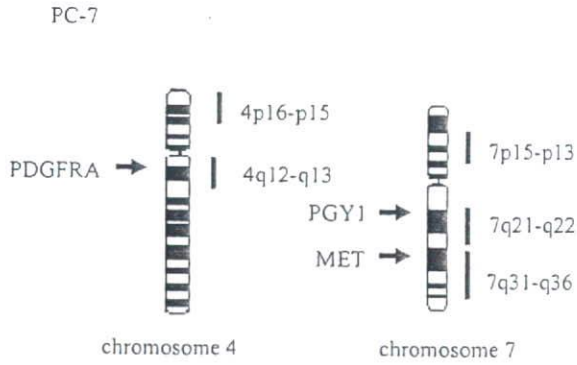

Fig. 3B　Gene and chromosome regions that showed amplification by CGH analysis and genomic DNA microarray in PC-7.

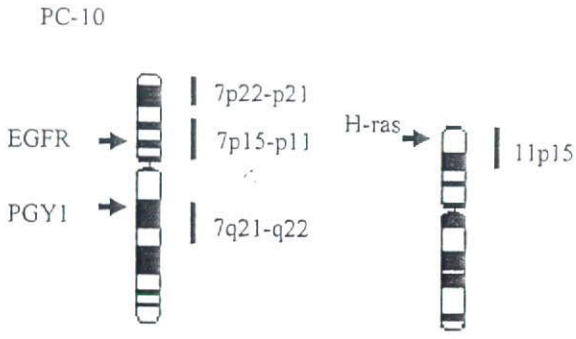

Fig. 3C　Gene and chromosome regions that showed amplification by CGH analysis and genomic DNA microarray in PC-10.

法はあくまでも個々の遺伝子のコピー数の変化をみるので、大変狭い範囲のDNA鎖に着目している。従ってCGH法で巨視的にみた場合に増幅のある領域でも、遺伝子レベルの狭い範囲に限定すると、増幅がない領域を含むこともある。従って、両者が必ずしも完全に一致するとは限らないと考えられた。

CGH法による解析結果でこれまで報告されている

肺癌に関与する癌遺伝子を複数の肺癌細胞株で認めた。その非小細胞肺癌における発現頻度はc-kit(4q12)は約5%未満、EGFR(7p12)は約40%[18-20]、c-Myc(8q24)は約30%、cyclinD1(11q13)は約50%。K-ras(12p12)は約15%の発現頻度という報告がある[21)22)]。また非小細胞肺癌における癌抑制遺伝子の発現頻度は、RASSF1A(3p21)は約40%、BLU(3p21)は約<10%、SEMA3B(3p21)は約50%、$p16^{INK4a}$、$p14^{ARF}$(9p21)は約40%、PTEN(10q23)は約<10%、PPP2R1B(11q23)は約15%、TSLC1(11q23)は約40%、LKB1/STK11(19p13)は約20%程度の発現頻度で認めるという報告がある[23)24)]。

CGH法に於いては、肺癌と関与があると今まで報告されている染色体異常領域にとどまらず、その他の領域においても肺癌との関与を疑わせるいくつかの領域を認めた。PC-3、PC-7、PC-14に認めた6p25はHER2増幅との関与が報告されている。PC-1、PC-10、PC-14に認めた7p22は大腸癌との関与が報告されている[25)26)]。いずれも固形癌であり肺癌との関与を疑わせる結果であった。

増幅をCGH法とgenomic DNA microarray法の二法で認めた遺伝子異常は、PDGFRA、EGFR、PGY1、MET、H-ras、PAK1であり、このうちEGFRは非小細胞肺癌の約40%に認めるという報告がある。肺癌は今まで報告されている癌遺伝子以外にPAK1、PGY1、H-ras、PDGFRA、METなどの癌遺伝子との関与を疑う結果となった。

CGH法とgenomic DNA microarray法の二法により腫瘍の共通増幅領域、共通欠失領域を同定しその腫瘍の癌遺伝子、癌抑制遺伝子の染色体上の存在部位を推定できる。またその解析結果より病理組織学的gradeと予後予測との相関や、抗癌剤による治療効果予測因子などの同定が可能となる可能性を秘めており、臨床の舞台に於いて、この二法による遺伝子解析応用が今後の肺癌治療におけるテーラーメイド化に貢献すると考えられた。

文　献

1) Sekido Y, Fong KM, Minna JD: Molecular genetics of lung cancer. Annu Rev Med **54**: 73-87, 2003
2) Osada H, Takahashi T: Genetic aterations of multiple tumor suppressor and oncogenes in the carcinogenesis and progression of lung cancer. Oncogene **21**: 7421-7434, 2002
3) O'Shaughnessy JA, Kellof GJ, Gordon GB, Dannenberg AJ, Hong WK, Fabian CJ, Sigman CC, Bertagnilli MM, Stratton SP, Lam S, Nelson GW, Meyskens FL, Alberts DS, Follen M, Rustgi AK, Papadimitrakopoulou V, Scardino PT, Gazdar AF, Wattenberg LW, Sporn MB, Sakr WA, Lippman SM, Von Hoff DD: Treatment and Prevention of intraepithelial neoplasia: an important target for accelerated new agent development. Clin Cancer Res **8**: 314-346, 2002
4) Testa JR, Liu Z, Feder M, Bell DW, Balsara B, Cheng JQ, Taguchi T: Advances in the analysis of chromosome alterations in human lung carcinomas. Cancer Genet Cytogenet **95**: 20-32, 1997
5) Taguchi T, Zhou JY, Feder M, Litwin S, Szanto K, Testa JR: Detection of aneuploidy in interphase nuclei form non-small cell lung carcinomas by fluorescence in situ hybridization using chromosome-specific repetitive DNA probes. Cancer Genet Cytogenet **89**: 120-125, 1996
6) Rodenhuis S, Slebos RJ: Clinical significance of ras oncogene activation in human lung cancer. Cancer Res **52**: 2665s-2669s, 1992
7) Brambilla E, Negoescu A, Gazzeri S, Lantuejoul S, Moro D, Barmbilla C, Coll JL: Apoptosis-related factors p53, Bcl2, and Bax in neuroendocrine lung tumors. Am J Pathol **149**: 1941-1952, 1996
8) Dammann R, Li C, Yoon JH, Chin PL, Bates S, Pfeifer GP: Epigenetic inactivation of a RAS association domain family protein from the lung tumor suppressor locus 3p21.3. Nat Genet **25**: 315-319, 2000
9) Ji L, Nishizaki M, Gao B, Burbee D, Kondo M, Kamibayashi C, Xu K, Yen N, Atkinson EN, Fang B, Lerman MI, Roth JA, Minna JD: Expression of several genes in the human chromosome 3p21.3 homozygous deletion region by an adenovirus vector results in tumor suppressor activites in vitro and in vivo. Cancer Res **62**: 2715-2720, 2002
10) Kallioniemi A, Kallioniemi OP, Sudar D, Rutovitz D, Gray JW, Waldman F, Pinkel D: Comparative genomic hybridization for molecular cytogenetic analysis of solid tumors. Science **30**: 818-821, 1992
11) Kallioniemi OP, Kallioniemi A, Piper J, Isola J, Waldman FM, Gray JW, Pinkel D: Optimizing comparative genomic hybridization for analysis of DNA sequence copy number changes in solid tumors. Genes Chromosomes Cancer **10**: 231-243, 1994
12) Kallioniemi A, Kallioniemi OP, Piper J, Tanner M, Stokke T, Chen L, Smith HS, Pinkel D, Gray JW, Waldman FM: Detection and mapping of amplified DNA sequence in breast cancer by comparative genomic hybridization. Proc Natl Acad Sci USA **91**: 2156-2160, 1994

13) DeRisi J, Penland L, Brown OP, Bittner ML, Meltzer PS, Ray M, Chen Y, Su YA, Trent JM : Use of a cDNA microarray to analyse gene expression patterns in human cancer. Nat Genet **14** : 457-460, 1996
14) 中村治彦、小高達朗、高橋英介、小林寿光、斉藤誠、高橋秀暢、松島　康、小中千守、加藤治文：長期継代が肺癌培養細胞株の性状に及ぼす影響。肺癌 **31** : 503-510, 1991
15) Daigo Y, Chin SF, Gorringe KL. Bobrow LG, Ponder BA, Pharoah PD, Calas C : Degenerate oligonucleotide primed-polymerase chain reaction-based array comparative genomic hybridaization for extensive amplicon profiling of breast cancers : a new approach for the molecular analysis of paraffin-embedded cancer tissue. Am J Pathol **158** : 1623-1631, 2001
16) Hui AB, Lo KW, Yin XL, Poon WS, Ng HK : Detection of Multiple Gene Amplifications in glioblastoma multiforme using array-based comparative genomic hybridization. Lab Invest **81** : 717-723, 2001
17) 中村治彦、佐治　久、保坂　誠、萩原　優、緒方昭彦、川崎徳仁、加藤治文：CGH と FISH で検出した肺癌染色体異常。Cytometory Research **11** : 9-14, 2001
18) Mendelsohn J, Baselga J : Status of epidermal growth factor receptor antagonists in the biology and treatment of cancer. J Clin Oncol **21** : 2787-2799, 2003
19) Scagliotti GV, Selvaggi G, Novello S, Hirsch FR : The biology of epidermal growth factor receptor in lung cancer. Clin Cancer Res **10** : 4227s-4232s, 2004
20) Shigematu H, Gazdar AF : Somatic mutations of epidermal growth factor receptor signaling pathway in lung cancers. Int J Cancer **118** : 257-262, 2006
21) Mills NE, Fishman CL, Rom WN, Dubin N, Jacobson DR : Increased prevalence of K-ras oncogene mutations in lung adenocarcinoma. Cancer Res **55** : 1444-1447, 1995
22) Noda N, Matuzoe D, Konno T, Kawahara K, Yamashita Y, Shirakusa T : K-ras gene mutations in non-small cell lung cancer in Japanese. Oncol Rep **8** : 889-892, 2001
23) Kuramochi M, Fukuhara H, Nobukuni T, Kanbe T, Maruyama T, Ghosh HP, Pletcher M, Isomura M, Onizuka M, Kitamura T, Sekiya T, Reeves RH, Murakami Y : TSLC1 is a tumor-suppressor gene in human non-small-cell lung cancer. Nat Genet **27** : 427-430, 2001
24) Carretero J, Medina PP, Pio R, Montuenga LM, Sanchez-Cespedes M : Novel and natural knockout lung cancer cell lines for the LKB1/STK11 tumor suppressor gene. Oncogene **23** : 4037-4040, 2004
25) Benachenhou N, Guiral S, Gorska-Flipot I, Labuda D, Sinnett D : High resolution deletion mapping reveals frequent allelic losses at the DNA mismatch repair loci hMLH1 and hMSH3 in non-small cell lung cancer. Int J Cancer **17** : 173-180, 1998
26) Osborne LR, Herbrick JA, Greavette T, Heng HH, Tsui LC, Scherer SW : PMS2-related genes flank the rearrangement breakpoints associated with Williams syndrome and other diseases on human chromosome 7. Genomics **45** : 402-406, 1997

Comparison analysis between comparative genomic hybridization and genomic DNA microarray of abnormalities of the genes in lung cancer cell lines

Akihiko OGATA[1], Haruhiko NAKAMURA[2], Makoto HOSAKA[1], Hisashi SAJI[1], Masaru HAGIWARA[1], Norihito KAWASAKI[1], Norihiko IKEDA[3], Harubumi KATO[1]

[1]First Department of Surgery, Tokyo Medical University
[2]Department of Thoracic Surgery, International University of Health and Welfare Atami Hospital
[3]Respiratory Disease Center, International University of Health and Welfare Mita Hospital

Abstract

We performed comparative analyses between comparative genomic hybridization (CGH) and genomic DNA microarray abnormalities of the genes in lung cancer cell lines. DNA was extracted from different lung cancer cell lines. All the lung cancer cell lines which we analyzed were non-small cell lung cancer cell lines established in our department. These were PC-1, PC-3, PC-7, PC-10 and PC-14. We performed gene analysis by CGH and genomic DNA microarray. DNA was extracted from the cell lines and the DNA chip used for this experiment had 59 kinds of gene probes. The common oncogenes detected by these two methods were PDGFRA, EGFR, PGY1, MET, H-ras and PAK1. The results by these two methods were identical in part, but not completely so. Therefore these two methods may be useful for analysis of abnormality of the genes in clinical cases.

〈**Key words**〉 comparative genomic hybridization (CGH), genomic DNA microarray, lung cancer cell line, oncogene, tumor suppressor gene

Detection & Diagnosis

発見・診断

ハイリスク患者の検診

池田 徳彦, 林 和, 岩崎 賢太郎

1 現行の肺癌検診

胸部単純レントゲンと高危険群に対する喀痰細胞診を用いた肺癌検診は欧米の大規模比較試験の結果，死亡率の減少効果なしと判断され[1,2]，以後，制度として存続しえなくなった．わが国では1990年代後半に胸部レントゲンと喀痰細胞診を用いた肺癌検診を症例対照研究の手法を用いて，死亡減少効果を評価した．その結果，質の高い精度管理の下に行われる肺癌検診は肺癌による死亡の抑制効果があることが証明された（表1）[3-6]．この研究が行われた地域は模範的な地域であり，わが国全体をながめると，現行の肺癌検診における受診率の低さや地域差，精度管理に対する意識の低さが問題となっている．この研究は高く評価されつつも，後ろ向きの研究デザインゆえ，海外での肺癌検診の否定的な意見を変えるには至っておらず，最近発刊されたACCPのガイドラインにおいても，胸部レントゲンと喀痰細胞診による肺癌検診は効果が無く推奨し得ないと述べられている[7]．

2 CTによる肺癌検診

従来，CTは胸部単純レントゲン検査に比べ，肺野の微小陰影の検出能に優れていることは知られていたが，撮影時間が長い，被曝量が多い，撮影コストが高いなどの点から検診への導入は困難であると考えられていた．しかし近年，低線量高速らせんCT（Helical scan CT）の出現により撮影時間は大幅に短縮され，被曝量を下げても良質な画像が得られるようになり，検診への導入が可能となった．国内外よりCTを肺癌検診に応用した報告が数多く出され，いずれも従来のレントゲンを用いた検診方法と比較して，肺癌の発

表1 日本における肺癌検診の症例対照研究

	方法	症例数		検診受診率		オッズ比 (95%CI)
		ケース	対照	ケース	対照	
宮城	X-P＋Sp	328	1,886	73.5	82.6	0.54 (0.41～0.73)
岡山	X-P＋Sp	412	3,490	32.3	43.9	0.59 (0.46～0.74)
新潟	X-P＋Sp	174	801	35.0	56.2	0.40 (0.27～0.59)
群馬	X-P	121	536	57.9	67.2	0.68 (0.44～1.05)

X-P: 胸部レントゲン
Sp: 喀痰

表2　代表的なCT検診の成績

報告者	症例数	年齢	肺癌発見率(%)	I期割合(%)	良性結節に対する精査数/CT検査陽性数(%)
Sobue	1,611	40~79	0.87	78	7
Sone	5,483	40~74	0.4	100	7.9
Nawa	7,956	50~69	0.44	89	1.7
Henschke	1,000	60~	2.5	83	26.2
Swensen	1,520	50~85	2.7	85	4

見率，とくにⅠ期の割合が飛躍的に増加したことが報告されている（表2）[8~11]．またInternational Early Lung Cancer Action Program（I-ELCAP）のCT検診で発見された肺癌の切除成績がきわめて良好であることが報告された[12]．1993年から2005年までの間にCT検診を受診した31,567人，このうち発見された肺癌症例484例を対象に検討した．発見肺癌の85%が病期Ⅰ期であり，10年生存率は88%（発見後1カ月以内の切除例では92%）であった．予後がきわめて良好な高分化腺癌がどの程度切除例に含まれていたかは定かではなく，過剰診断をはじめとするバイアスにより生存率が見かけ上，向上している可能性は否定できない．しかし，バイアスのみでこの驚異的な成績が説明し得ないのも事実であり，肺癌の高リスクを有する個人にとっては朗報であろう．

欧米ではCT検診により肺癌による死亡が減少するか否か評価するため，前向きの比較試験が行われている．米国ではNCI（National Cancer Institute）主導によるNational Lung Screening Trialが行われている．2002年より5万人規模の胸部レントゲンによる検診とCT検診の無作為比較試験により肺癌の死亡抑制効果を評価する．登録は2004年2月に終了し，2009年まで追跡調査を行う．ヨーロッパにおいても，フランスでは胸部レントゲン検診とCT検診を比較したDepiscan，オランダ，ベルギーではCT検診と非検診を比較したNelson Trialなどの研究が行われている．

3　CT検診に対する評価

CT検診の標準化とあるべき姿を示すために2004年に日本肺癌学会と日本CT検診学会が中心となり，低線量CTによる肺癌検診の手引きを刊行した[14]．これにより現時点での検診対象，検診間隔，検診方法，精度基準や精査のあり方が記載されている．平成17年度がん研究助成金「がん検診の適切な方法とその評価法の確立に関する研究」班（主任研究者　祖父江友孝）では国内外の1663編の論文を抽出しEBMの手法により「有効性評価に基づく肺癌検診ガイドライン」を作成し，公開している[15]．これによれば非高危険群に対する胸部X線検査，および高危険群に対する胸部X線検査と喀痰細胞診併用法による肺癌検診は死亡率減少効果を示す直接的証拠を認めるので対策型および任意型検診として実施することを勧めるとしている．一方，低線量CTによる検診は現時点では試行的研究であり対策型検診として採用するには時期尚早としている．CT検診における不利益として，高い被曝線量とともに，多くの良性病変を精査することになる点があげられる（表2）．気管支鏡，経皮的針生検あるいは胸腔鏡による検査は侵襲的であり，なおかつ相応の合併症が発生する．検診による死亡減少効果が不明であることに加え，これらの重大な不利益に関して説明する必要がある．

ACCPのガイドラインにおいても，低線量CTによる肺癌検診は治験に参加する以外は推奨し得ないと述べられている[7]．読影医の負担軽減策としてcomputer-aided diagnosis（CAD）による読影支援や一次読影を担当するスクリーナー構想も検討されている[16]．

4 CT検診の応用

肺癌のみならず，慢性閉塞性肺疾患の評価と禁煙支援を行うプログラムを実践している施設もある．腹部のCTスライスを追加することにより内臓脂肪の量を測定しメタボリックシンドロームの程度を評価することも試みられている．また，じん肺をはじめとする職業性呼吸器病に関しては従来より国際労働機関が規定したX線分類により評価されていたが，客観性や再現性に乏しい点も指摘されており，国内外でCTを適用する傾向である[17]．アスベスト曝露労働者を対象として胸部CTによるスクリーニングを行ったフィンランドからの報告では，肺癌や胸膜プラークを発見したが悪性胸膜中皮腫を発見したという記述はなく[18]，CTを用いて悪性胸膜中皮腫を対象とした検診を行うことは今後の検討事項であろう．

結　語

2007年10月に刊行された米国胸部疾患学会のガイドライン（第2版）では「CT検診によりⅠ期の肺癌の発見率は上昇し，発見された肺癌の切除成績も良好であることは周知の事実である．しかし良性病変に対して本来不必要な検査や手術をすることに対するリスクや経済的負担，患者の精神的負担などは未解決のままである．前向きの比較試験で明確な結論が得られるまでは，CTを標準的な検診方法として推奨し得ない．」というものである[7]．一方，CTの普及により小型肺癌の発見が著しく増加し，このような特殊な肺癌を解析することにより発癌過程あるいは癌の本態を解明する手がかりとなる可能性がある．CT検診自体の評価は比較試験の結果待ちの様相であるが，小型肺癌の解析を通して肺癌研究の進歩が加速しつつあるのが現状である．

文　献

1) Melamed MR, Flehinger BJ, Zaman MB, et al: Screening for early lung cancer: results of the Memorial Sloan-Kettering study in New York. *Chest* 86: 44-53, 1984
2) Fontana R, Sanderson DR, Woolner LB, et al: Lung cancer screening: the Mayo program. *J Occup Med* 28: 746-750, 1986
3) Nishii K, Ueoka H, Kiura K, et al: A case-control study of lung cancer screening in Okayama Prefecture, Japan. *Lung Cancer* 34: 325-332, 2001
4) Tsukada H, Kurita Y, Yokoyama A, et al: An evaluation of screening for lung cancer in Niigata Prefecture, Japan: A population-based case-control study. *Br J Cancer* 85: 1236-1331, 2001
5) Nakayama T, baba T, Suzuki T, et al: An evaluation of chest X-ray screening for lung cancer in gunma prefecture, Japan: a population-based case-control study. *Eur J Cancer* 38: 1380-1387, 2002
6) Sagawa M, Tsubono Y, Saito Y, et al: A case-control study for evaluating the efficacy of mass screening program for lung cancer in Miyagi Prefecture, Japan. *Cancer* 92: 588-594, 2001
7) ACCP Evidence-Based Clinical Practice Guidelines (2nd Edition). *Chest* (Supplement) 132: 69S-77S, 2007
8) Sone S, Takashima S, Li F, et al: Mass screening for lung cancer with mobile spiral computed tomography scanner. *Lancet* 351: 1242-1245, 1998
9) Kaneko M, Eguchi K, Ohmatsu H, et al: Peripheral lung cancer: screening and detection with low-dose spiral CT versus radiography. *Radiology* 201: 798-802, 1996
10) Nawa T, Nakagawa T, Kusano S, et al: Lung cancer screening using low-dose spiral CT- results of baseline and one-year follow-up studies. *Chest* 122: 15-20, 2002
11) Henschke C, McCauley D, Yakelevitz D, et al: Early Lung Action Project: overall design and findings from baseline screening. *Lancet* 354: 99-105, 1999
12) The International Early Lung Cancer Action Program: Investigators Survival of Patients with Stage Ⅰ Lung Cancer Detected on CT Screening. *NEJM* 355: 1763-1771, 2006
13) 厚生労働省科学研究費補助金　第3次対がん総合戦略研究事業　革新的な診断技術を用いたこれからの肺がん検診手法の確立に関する研究（CT肺がん検診有効性コホート研究・喀痰細胞診有効性症例対照研究）主任研究者

鈴木隆一郎：平成17年度総括・分担研究報告書
14) 低線量CTによる肺癌検診のあり方に関する合同委員会：低線量CTによる肺癌検診の手引き，金原出版，東京，2004
15) 平成17年度がん研究助成金「がん検診の適切な方法とその評価法の確立に関する研究」班（主任研究者　祖父江友孝）：http: //canscreen. ncc. go. jp/index. html
16) 花井耕造：胸部CTスクリーナー制度の構築について，CT検診 13: 8, 2006
17) Suganuma N, Kusaka Y, Hiraga Y, et al: Asbestos-Related Pleural Abnormalities Detected by Chest X-Ray : Fair Agreement with Detection by Computed Tomography. *J Occup Health* 43: 365-370, 2001
18) Tiitola M, Kivisaari L, Huuskonen MS, et al: Computed tomography screening for lung cancer in asbestos-exposed workers. *Lung Cancer* 35: 17-22, 2002

Radiotherapy and Oncology 86 (2008) 258–263
www.thegreenjournal.com

Postal dosimetry

Feasibility study of glass dosimeter postal dosimetry audit of high-energy radiotherapy photon beams

Hideyuki Mizuno[a,*], Tatsuaki Kanai[a], Yohsuke Kusano[b], Susumu Ko[a], Mari Ono[c], Akifumi Fukumura[a], Kyoko Abe[d], Kanae Nishizawa[a], Munefumi Shimbo[e], Suoh Sakata[f], Satoshi Ishikura[g], Hiroshi Ikeda[g]

[a]*Research Center for Charged Particle Therapy, National Institute of Radiological Sciences, Chiba, Japan,* [b]*Accelerator Engineering Corporation, Chiba, Japan,* [c]*Keio University Hospital, Tokyo, Japan,* [d]*Toho University Graduate School, Funabashi, Japan,* [e]*Saitama Medical Center, Kawagoe, Japan,* [f]*Association for Nuclear Technology in Medicine, Tokyo, Japan,* [g]*National Cancer Center, Tokyo, Japan*

Author

Introduction: The characteristics of a glass dosimeter were investigated for its potential use as a tool for postal dose audits. Reproducibility, energy dependence, field size and depth dependence were compared to those of a thermoluminescence dosimeter (TLD), which has been the major tool for postal dose audits worldwide.

Materials and methods: A glass dosimeter, GD-302M (Asahi Techno Glass Co.) and a TLD, TLD-100 chip (Harshaw Co.) were irradiated with γ-rays from a ^{60}Co unit and X-rays from a medical linear accelerator (4, 6, 10 and 20 MV).

Results: The dosimetric characteristics of the glass dosimeter were almost equivalent to those of the TLD, in terms of utility for dosimetry under the reference condition, which is a 10×10 cm^2 field and 10 cm depth. Because of its reduced fading, compared to the TLD, and easy quality control with the ID number, the glass dosimeter proved to be a suitable tool for postal dose audits. Then, we conducted postal dose surveys of over 100 facilities and got good agreement, with a standard deviation of about 1.3%.

Conclusions: Based on this study, postal dose audits throughout Japan will be carried out using a glass dosimeter.
 Radiotherapy and Oncology 86 (2008) 258–263.

Keywords: Postal dose audit; Glass dosimeter; Reference condition

Thermoluminescence dosimeters (TLD) have been used as the standard tool for dose audits for the past few decades [1,5,9,10]. They have good reproducibility and small energy dependence [12,13]. However, TLD powder requires careful handling and fading correction. On the other hand, glass dosimeters are almost free from the fading effect and can be read repeatedly [15]. They have been used for personal radiation monitoring for a long time. However, the problems of its high pre-dose and energy dependence prevented this tool from becoming an alternative to TLD [15]. Recently, a new type of glass rod dosimeter has become commercially available, which achieves great improvement in the reading method to avoid pre-dose effect [4]. Tsuda [17] reported its reproducibility as 0.82% in the coefficient of variance, which is comparable that of to TLD. Furthermore, good linearity, up to 10 Gy, and less fading, 1.90% after 129 days, were also achieved. Araki et al. [2] used a glass dosimeter to measure the Gamma-Knife helmet output factors and gave an indication of its superiority over TLD. They [3] also applied the glass dosimeter to linac beams of several energies and achieved slight energy dependencies within 2%. The glass dosimeter's energy dependence is not a serious impediment to dosimetry under reference conditions.

Regarding the audit system, IAEA/WHO, the Radiological Physics Center (RPC) and the European Society for Therapeutic Radiology and Oncology (ESTRO) have performed postal dose audits worldwide or nationwide [1,5,6,9–11]. However, Japan has not yet been included in any audit group. In Japan, only a few pilot studies have been done [7]. Shimbo et al. [16] developed the postal dose audit system using a glass dosimeter. We are now on a project to establish a permanent dose audit system based on their system. Glass dosimeters have the potential to become the next generation of detectors for the audit system because of their handling advantage, reduced fading (relative to TLD) and repeatable readout. In this article, we report the comparison between a glass dosimeter and TLD as the tool for postal audits, focusing on its application to reference condition dosimetry. In addition, the results of the pilot postal audit study are shown, which was conducted at over 100 radiotherapy facilities.

0167-8140/$ - see front matter doi:10.1016/j.radonc.2007.10.024

Materials

Glass dosimeter

The glass dosimeter (DOSE ACE, Asahi Techno Glass Corporation; ATG) is silver-activated phosphate glass. Its weight composition is as follows: 11.0% Na, 31.55% P, 51.16% O, 6.12% Al and 0.17% Ag [17]. Though it is not the tissue-equivalent material, it does not affect our application such as relative dosimetry between our standard dose and the dose of certain hospital. Its dimensions are 1.5 mm in diameter and 12 mm in length. ID number is engraved for each element. It is based on radiophotoluminescence (RPL). Radiations produce RPL centers, which emit orange luminescence by UV-ray excitation. After emitting the luminescence, they will return to the stable RPL centers. Therefore, the numbers of RPL centers stay constant, allowing infinite numbers of readings for the same irradiation. In this study, outputs of glass dosimeters were average of five times sequential reading. The RPL centers are cleared by annealing (400 °C with 30 min), so that we can use the element sequentially. An FDG-1000 (ATG) was used as a reader.

The major dosimetric features taken into account were reproducibility and energy dependence. The reproducibility of the RPL signal depends on the element's cutting precision and UV-ray output stability. As for energy dependence, the mass energy absorption coefficient of the glass dosimeter, silver-activated metaphosphate, is several times higher than that of TLD, LiF, for low energy photons around 25 keV (see Fig. 1). This can affect the energy dependence factor.

Thermoluminescent dosimeter

The thermoluminescent dosimeter (TLD-100, Harshaw) is lithium fluoride doped with magnesium and titanium. Several forms are provided such as powders, chips, rods and cubes. Absorbed energy is stored in the crystal lattice, which results in visible light emission by heating. Because of its good physical aspects, including size, tissue-equivalent composition and fine reproducibility, the TLD-100 has been widely used as a postal dose audit tool. We used a chip type with a size of 3.2 mm × 3.2 mm × 0.9 mm. The reader was a Harshaw 5500. The reading temperature is from 50 to 400 °C in order to accumulate the main peak (~210 °C) of glow curve. Annealing was done by the combination of 400 °C for 1 h and 100 °C for 2 h.

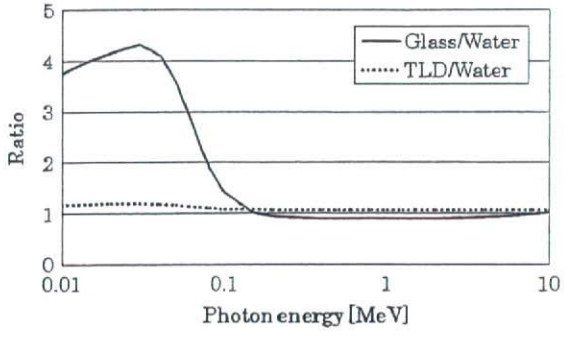

Fig. 1. The ratio of mass energy absorption coefficient between glass dosimeter (silver-activated metaphosphate)/TLD (LiF) and water (acquired from NIST database [14]).

Tough water phantom

A water equivalent solid phantom, called the tough water phantom (Kyoto Kagaku Co.), was used. It consists mainly of C, O and H. Its density, mean atomic number and electron density are 1.01 g/cm^3, 7.42 and 3.25×10^{23}/cm^3, respectively. Those of water are 1.00 g/cm^3, 7.42 and 3.34×10^{23}/cm^3, respectively. Its size was 30 cm × 30 cm, it was a slab type and its central region was gouged to contain the glass dosimeters and TLDs.

Investigation of dosimetric characteristics

Experiments

Reproducibility

Reproducibility was examined for both dosimeters, glass dosimeter and TLD, using ^{60}Co γ-rays (Yoshizawa-LA, TYC-3001) and linac X-rays (Varian, Clinac21EX; 6 MV, 10 MV). Dosimeters were set at a reference depth of 10 cm in the tough water phantom (Fig. 2). Field size was 16 cm ϕ for ^{60}Co γ-rays and 10 × 10 cm^2 for X-rays. For each beam, 15 elements were irradiated uniformly. Each element's output was corrected with its own sensitivity. Corrected outputs were divided by the average of 15 elements' output. The measurement cycle, from irradiation to annealing, was done three times to decrease the statistical error.

Energy dependence of glass dosimeter

Energy dependence was examined for the glass dosimeter using ^{60}Co γ-rays and linac X-rays (Mitsubishi, EXL-15DP; 4 MV, Varian, Clinac21EX; 6 MV, 10 MV and Clinac23EX; 20 MV). The experimental setup was the same as in Fig. 2, and the measurements using the ionization chamber were taken under the same conditions. The stability of the output of ^{60}Co γ-rays or linac X-rays was much less than 1%. Measurements were done several times to decrease the statistical error. For each measurement, at least 10 elements were used for one energy.

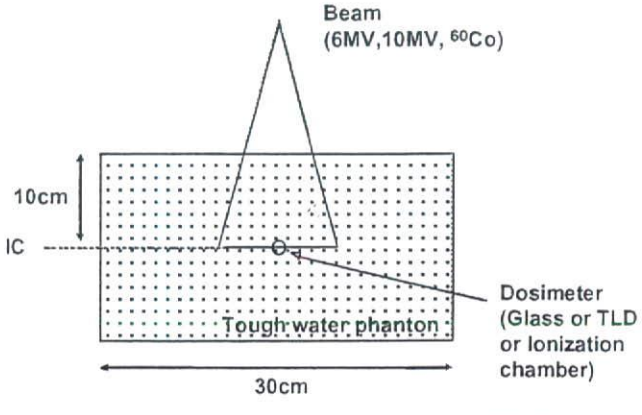

Fig. 2. Setup of reproducibility and energy dependence experiments; dosimeters were placed at 10 cm depth in the isocenter (IC).

The protocol used to determine the absolute dose was the Japanese code, Standard Dosimetry of Absorbed Dose in External Beam Radiotherapy (Standard Dosimetry 01), which is based mainly on IAEA Technical Reports Series No. 398.

Field size and depth dependence

To examine the glass dosimeter's response to low energy photons, field size and depth were changed, because the mean beam energy fell with increasing field size and decreasing depth. Both dosimeters, glass dosimeter and TLD, were irradiated using linac X-rays (Varian, Clinac21EX; 6 MV, 10 MV). Measurements were done at 5×5, 10×10 and 20×20 cm^2 field sizes and at the D_{max} (1.5 cm for 6 MV and 2.5 cm for 10 MV), 5, 10 and 20 cm depth in the tough water phantom. For each condition, 5 elements of glass dosimeter and 3 elements of TLD were used. Once again, the measurements using the ionization chamber were also done under the same condition, that is, measured in tough water phantom.

Results and discussion

Reproducibility

The deviations obtained from both the TLD and the glass dosimeter are shown in Fig. 3. The standard deviation was 0.8% for the glass dosimeter. This value is comparable to the TLD value, 0.7%.

Energy dependence of glass dosimeter

The obtained energy correction factor is shown in Table 1. They were represented as

$$E_q = \frac{\text{Glass(Co)}/D_{med}(\text{Co})}{\text{Glass}(q)/D_{med}(q)}$$

where Glass(Co)/D_{med}(Co) is the light output per unit dose in a medium for ^{60}Co γ-rays. Glass(q)/D_{med}(q) is the light output per unit dose in the same medium for the beam quality q of interest. Beam quality q is represented as $TPR_{20,10}$. The glass dosimeter had a slightly positive correlation with beam energy. However, for the mega-voltage region, the levels of dependence were equivalent to those of the TLD achieved by IPSM [8,13] within the experimental errors. Their TLD factor was obtained by exchanging the glass dosimeter output to the TLD output of above equation.

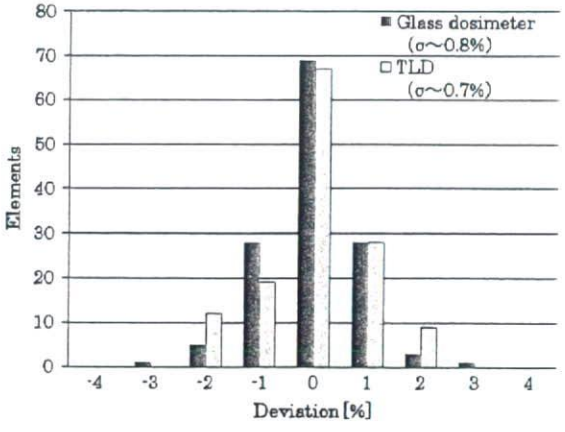

Fig. 3. Reproducibility of glass dosimeter and TLD; 45 elements were repeatedly irradiated by ^{60}Co, 6 and 10 MV X-rays.

Table 1
Quality dependence of glass dosimeter in photon beams by experiment

Energy (MV)	$TPR_{20,10}$	Glass dosimeter factor (E_q)	TLD factor (IPSM 1990, [7,10])
^{60}Co γ-rays	0.58	1.000	1.000
4	0.624	1.007 ± 0.005	
6	0.669	1.014 ± 0.009	1.011
10	0.740	1.026 ± 0.007	1.023
20	0.791	1.029 ± 0.004	

Field size and depth dependence

The obtained ratios of readings from the glass dosimeter/TLD to ionization chamber outputs are shown in Fig. 4. The values were normalized at reference conditions, 10×10 cm^2 field and 10 cm depth. The ratios for the glass dosimeter were from 0.975 to 1.011 (mean 0.995) for 6 MV, and from 0.973 to 1.031 (mean 0.999) for 10 MV. Those for TLD were from 0.971 to 1.018 (mean 0.996) for 6 MV and from 0.985 to 1.038 (mean 1.014) for 10 MV.

The outputs of the glass dosimeter became slightly smaller, from 1.7 to 2.7%, for a 5×5 cm^2 field compared to 10×10 cm^2 and 20×20 cm^2 fields. This might have been caused by the change in energy spectrum. The mean energy of X-rays becomes higher in the smaller field because of the decrease in scattered photons within the field. However, overall, it seems that the ratios of the glass dosimeter were almost at the same level, or were rather stable, compared to the TLD, for changes in both field size and depth.

Discussion for the dosimetric properties

Even for non-reference dosimetry, glass dosimeter proved to be a potential alternative to TLD. Moreover, the glass dosimeter has the advantage of less fading. In the postal dose audit process, control elements are used to calibrate the reader. Known doses are irradiated onto the control elements by the audit director. Some audit groups irradiate the control elements at only the same timing as the intended facility's irradiation, to minimize the fading effect. By using glass dosimeter, this kind of limitation regarding fading becomes more flexible.

Postal dose audit trial

We conducted a pilot postal audit at over 100 radiation therapy facilities to verify the overall feasibility of establishing a postal dose audit system using glass dosimeters.

Postal tools

We sent 20 glass elements and one set of solid phantoms to participating facilities. The glass dosimeters were contained in tough water phantom (Fig. 5).

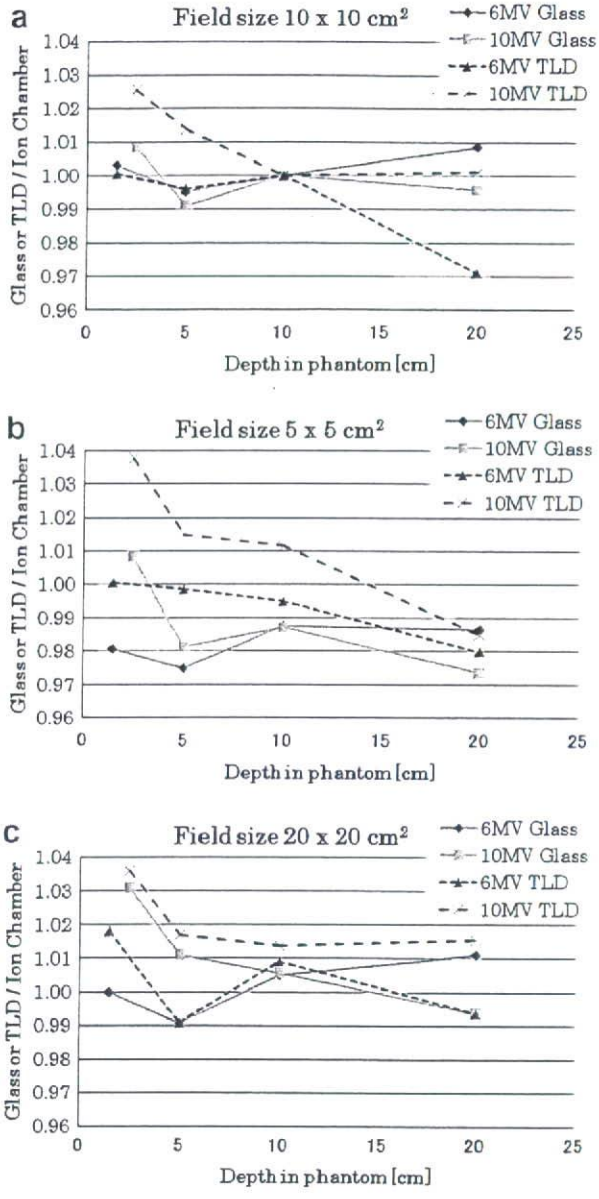

Fig. 4. Ratios between glass dosimeter/TLD and ionization chamber outputs for different field sizes and depths. The field sizes were (a) 10×10 cm^2, (b) 5×5 cm^2, (c) 20×20 cm^2, respectively. The values were normalized at reference conditions, 10×10 cm^2 field and 10 cm depth. The uncertainties of each measured value were 1.5% in standard deviation for glass dosimeter and 1.6% for TLD.

The assignments for the 20 glass elements are shown in Table 2. Twelve elements were "audit elements" that were irradiated with X-rays by a participant (six elements for each of two X-ray energies), six elements were "control elements" that were irradiated with a ^{60}Co beam at NIRS, and two elements were "background elements" that were not irradiated during the audit process. "Control elements" were used to calibrate the reader's sensitivity. These assignments were adopted to minimize the statistical error in final reading outputs under the limitation of the number of sequential readings, 20 elements for one reading run.

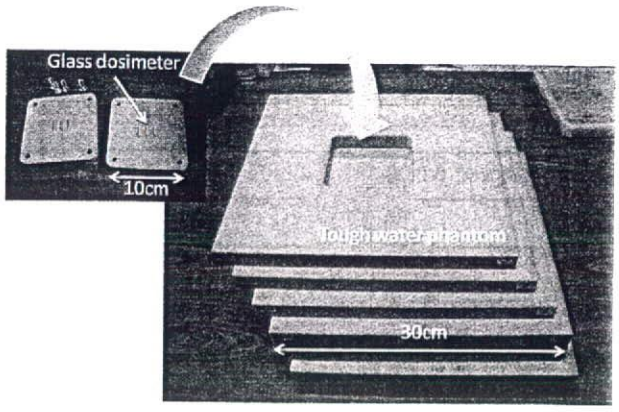

Fig. 5. Glass dosimeter and tough water phantom; tough water phantom is gouged to contain the glass dosimeters.

Table 2
Assignment of one set of glass dosimeters (20 elements)

Name	Element ID	Irradiation condition
Audit elements	Nos. 1–6	1 Gy is irradiated by applied facility by energy 1
	Nos. 7–12	1 Gy is irradiated by applied facility by energy 2
Control elements	Nos. 13–18	1 Gy is irradiated by NIRS by ^{60}Co
Background elements	Nos. 19 & 20	No irradiation

Determination of absorbed dose

The method this audit used to derive the output of irradiation dose to the glass dosimeters is shown below.

1. Twenty elements were read (one run).
2. We repeated the run five times. The rotation or position shifts of the element set in the reader were checked before each run.
3. Outputs of five runs were averaged for each element.
4. We multiplied by the following correction factors (definitions are shown later)
   - Elements' sensitivity correction factor
   - Energy correction factor
   - Phantom correction factor.
5. We averaged the six elements irradiated at the same energy.
6. We determined the calibration ratio between the output of the glass dosimeter and the ionization chamber from the ^{60}Co irradiated data.
7. We multiplied the calibration ratio by the audited elements' output.

The applied facility's final output was defined as in the following equation.

$$D = \sum_{i=1}^{6}(X_i \times I_i) \times E_q \times P_q \times \frac{\mathrm{Dose}_{^{60}\mathrm{Co}}}{\sum_{i=13}^{18}(X_i \times I_i)}$$

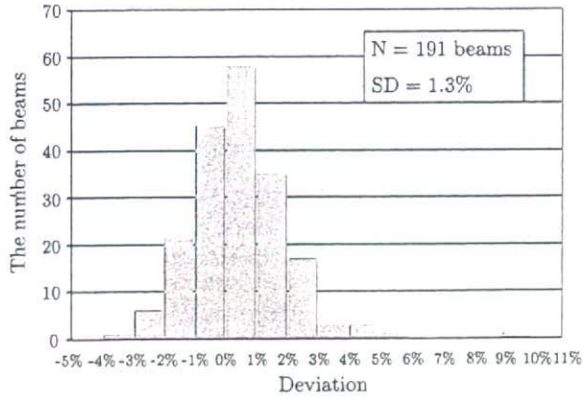

Fig. 6. The result of the postal dose audit for the 191 beams from 4 to 20 MV.

Table 3
Results of first and second postal dose audits

Facility	Beam quality (MV)	Deviation of audit		Probable causes
		First (%)	Second (%)	
A	4	4.1	1.9	Miscalculation of monitor unit
	10	9.2	0.9	(excluded daily MU calibration factor)
B	4	5.7	2.8	Mistake in measurement setup
	10	4.7	3.4	Mistake in calibration factor Substantial change in barometric pressure Uncalibrated thermobarometer
C	4	4.6	2.0	Unclear
	6	2.6	2.1	(Energy switching operation error?)

X_i is the raw output value of the glass element whose ID number is i, I_i is sensitivity correction factor of the glass element whose ID number is i (derived by uniform irradiation using ^{60}Co γ-rays).

$$I_i = \frac{D_{60_{Co}}}{X_i}$$

E_q is the energy correction factor of beam quality "q" (glass elements were irradiated by ^{60}Co γ-rays and 4, 6 and 10 MV X-rays. Correction factor was derived by using the output of the ionization chamber (IC), $D(^{60}\mathrm{Co})$ and $D(q)$, which were measured at the same setup as the glass dosimeter).

$$E_q = \left[\frac{\sum_i X_i(^{60}\mathrm{Co}) \times I_i}{\sum_i X_i(q) \times I_i}\right]^{\mathrm{Glass}} \times \left[\frac{D(q)}{D(^{60}\mathrm{Co})}\right]^{\mathrm{IC}}$$

P_q is the phantom correction factor of beam quality "q."

$$P_q = \frac{D_w}{D_T}$$

D_w is the output of the ionization chamber irradiated by X-rays of beam quality "q" in 10 cm deep water, D_T is the output of the ionization chamber irradiated by X-rays of beam quality "q" 10 cm deep in the tough water phantom, $\mathrm{Dose}_{60_{Co}}$ is the output of the ionization chamber irradiated by ^{60}Co γ-rays just before the irradiation of control elements (ID Nos. 13–18) with same setup.

I_i was assigned to each element to increase the outputs' precision. Of course, I_i, E_q and P_q were determined before the audit trial started. Accumulated uncertainty of each parameter was estimated to be 1.6% in one standard deviation.

Results of postal dose audit trial

We conducted the postal dose audit at 106 facilities using 191 beams. Seventy-seven beams were 4 MV, 31 beams were 6 MV, 81 beams were 10 MV, 1 beam was 14 MV and 1 beam was 20 MV. Fig. 6 shows the overall results of the outputs. The central value was 0.3% and standard deviation was 1.3%; 182 beams (95%) were within ±3%.

One facility showed a big deviation of over 9%. A second postal audit was conducted there, followed by an immediate hearing by phone. Finally, the apparent discrepancy was proved to arise from a participant's miscalculation of a monitor unit (excluding the correction factor of daily monitor chamber response). The result of the second postal audit at that facility was within 2%. Two other facilities, which showed deviations of more than 4%, also underwent a second postal audit. Those results are illustrated in Table 3. Clearly, the results were improved by the second audit, which showed the importance of external audits.

According to the ESTRO/EQUAL postal audit system [5], the optimum level is within ±3%, tolerance level is within ±5% and emergency level is over ±10% deviation. We followed these criteria to report the results to each facility. From this point of view, the reference dose is properly managed by these participants. In addition, glass dosimeters proved to be a suitable tool for postal dose audits.

Conclusion

The dosimetric features of glass dosimeters were examined and compared to those of TLD as tools for postal dose audits. Reproducibility and energy dependence were the same as in the TLD. Additionally, field size and depth dependence were at the same level, and were rather stable. Regarding handling advantages, repeatable readings and low fading, the glass dosimeter is likely to be a suitable tool for postal dose audits. Based on these results, and to check the overall system, we conducted a pilot postal audit at radiotherapy facilities. We got excellent results, in that the central value of the deviation was 0.3% and the standard deviation was 1.3%. A permanent postal dose audit system using glass dosimeters is therefore about to begin in Japan.

Acknowledgments

The postal audit was partially supported by a grant from the Ministry of Health, Labour and Welfare in Japan. The authors express

their thanks to the staff of the NIRS and AEC for their support of glass dosimeter irradiation and reading.

* **Corresponding author. Hideyuki Mizuno**, Research Center for Charged Particle Therapy, National Institute of Radiological Sciences, 4-9-1 Anagawa, Inage-ku, Chiba 263-8555, Japan. *E-mail address:* h_mizuno@nirs.go.jp

Received 16 August 2007; received in revised form 16 October 2007; accepted 17 October 2007; Available online 26 November 2007

References

[1] Aguirre JF, Tailor R, Ibbott G, Stovall M, Hanson, W. Thermoluminescence dosimetry as a tool for the remote verification of output for radiotherapy beams: 25 years of experience. In: Proceedings of the international symposium on standards and codes of practice in medical radiation dosimetry IAEA-CN-96/82. Vienna: IAEA; 2002. p. 191–99.

[2] Araki F, Ikegami T, Ishidoya T, Kubo HD. Measurements of Gamma-Knife helmet output factors using a radiophotoluminescent glass rod dosimeter and a diode detector. Med Phys 2003;30:1976–81.

[3] Araki F, Moribe N, Shimonobou T, Yamashita Y. Dosimetric properties of radiophotoluminescent glass rod detector in high-energy photon beams from linear accelerator and Cyber-Knife. Med Phys 2004;31:1980–6.

[4] Asahi Techno Glass Corporation. Explanation material of RPL glass dosimeter: small element System, Tokyo, Japan; 2000.

[5] Ferreira IH, Dutreix A, Bridier A, Chavaudra J, Svensson H. The ESTRO-QUALity assurance network (EQUAL). Radiother Oncol 2000;55:273–84.

[6] Kroutilíková D, Novotný J, Judas L. Thermoluminescent dosimeters (TLD) quality assurance network in the Czech Republic. Radiother Oncol 2003;66:235–44 .

[7] Hayami A, Inoue T, Kawagoe Y, Fuchihata H. Mailed TLD dose intercomparison at a reference point of high energy photon beams among 11 institutions in Japan. J Jpn Soc Ther Radiol Oncol 1997;9:139–45.

[8] Institute of Physical Science in Medicine (IPSM). Code of practice for high-energy photon therapy dosimetry based on the NPL absorbed dose calibration service. Phys Med Biol 1990;35:1355–60.

[9] Izewska J, Andreo P. The IAEA/WHO TLD postal programme for radiotherapy hospitals. Radiother Oncol 2000;54:65–72.

[10] Izewska J, Andreo P, Vatnitsky S, Shortt KR. The IAEA/WHO TLD postal dose quality audits for radiotherapy: a perspective of dosimetry practices at hospitals in developing countries. Radiother Oncol 2003;69:91–7.

[11] Izewska J, Georg D, Bera P, Thwaites D, Arib M, Saravi M, et al. A methodology for TLD postal dosimetry audit of high-energy radiotherapy photon beams in non-reference conditions. Radiother Oncol 2007;84:67–74.

[12] Kirby TH, Hanson WF, Johnston DA. Uncertainty analysis of absorbed dose calculations from thermoluminescence dosimeters. Med Phys 1992;19:1427–33.

[13] Mobit PN, Mayles P, Nahum AE. The quality dependence of LiF TLD in megavoltage photon beams: Monte Carlo simulation and experiments. Phys Med Biol 1996;41:387–98.

[14] National Institute of Standards and Technology (NIST). Tables of X-ray mass attenuation coefficients and mass energy-absorption coefficients from 1 keV to 20 MeV for elements $Z = 1$ to 92 and 48 additional substances of dosimetric interest. NISTIR 5632 (Version 1.4); 2004.

[15] Piesch E, Burgkhardt B, Vilgis M. Photoluminescence dosimetry: progress and present state of art. Radiat Prot Dosim 1990;33:215–26.

[16] Shimbo M, Nishio T, Ooyama M, et al. Report of the off-site dosimetry. Jpn J Med Phys 2003;23:25–6.

[17] Tsuda M. A few remarks on photoluminescence dosimetry with high energy X-rays. Jpn J Med 2000;20:131–9.

Int. J. Radiation Oncology Biol. Phys., Vol. 72, No. 1, pp. 144–152, 2008

0360-3016/08/$–see front matter

ELSEVIER

doi:10.1016/j.ijrobp.2007.12.047

CLINICAL INVESTIGATION **Radiation Oncology Practice**

JAPANESE STRUCTURE SURVEY OF RADIATION ONCOLOGY IN 2005 BASED ON INSTITUTIONAL STRATIFICATION OF PATTERNS OF CARE STUDY

TERUKI TESHIMA, M.D.,* HODAKA NUMASAKI, M.S.,* HITOSHI SHIBUYA, M.D.,† MASAMICHI NISHIO, M.D.,‡ HIROSHI IKEDA, M.D.,§ HISAO ITO, M.D.,¶ KENJI SEKIGUCHI, M.D.,‖ NORIHIKO KAMIKONYA, M.D.,# MASAHIKO KOIZUMI, M.D.,** MASAO TAGO, M.D.,†† YASUSHI NAGATA, M.D.,‡‡ HIDEKAZU MASAKI, M.D.,§§ TETSUO NISHIMURA, M.D.,¶¶ SHOGO YAMADA, M.D.,‖‖ AND JAPANESE SOCIETY OF THERAPEUTIC RADIOLOGY AND ONCOLOGY DATABASE COMMITTEE

* Department of Medical Physics and Engineering, Osaka University Graduate School of Medicine, Suita, Osaka, Japan; † Department of Radiology, Tokyo Dental and Medical University, Tokyo, Japan; ‡ Department of Radiology, National Hospital Organization Hokkaido Cancer Center, Sapporo, Hokkaido, Japan; § Division of Radiation Oncology, National Cancer Center, Tokyo, Japan; ¶ Department of Radiology, Chiba University Graduate School of Medicine, Chiba, Japan; ‖ Department of Radiation Oncology, St. Luke's International Hospital, Tokyo, Japan; # Department of Radiology, Hyogo College of Medicine, Nishinomiya, Hyogo, Japan; ** Department of Radiological Technology, Fujita Health University School of Health Sciences, Nagoya, Aichi, Japan; †† Department of Radiology, University of Tokyo Hospital, Tokyo, Japan; ‡‡ Department of Radiation Oncology and Image-Applied Therapy, Kyoto University Graduate School of Medicine, Kyoto, Japan; §§ Department of Radiology, National Center for Child Health and Development, Tokyo, Japan; ¶¶ Division of Radiation Oncology, Shizuoka Cancer Center, Shizuoka, Japan; and ‖‖ Tohoku University Hospital Cancer Center, Sendai, Japan

Purpose: To evaluate the structure of radiation oncology in Japan in terms of equipment, personnel, patient load, and geographic distribution to identify and improve any deficiencies.

Methods and Materials: A questionnaire-based national structure survey was conducted between March 2006 and February 2007 by the Japanese Society of Therapeutic Radiology and Oncology. These data were analyzed in terms of the institutional stratification of the Patterns of Care Study.

Results: The total numbers of new cancer patients and total cancer patients (new and repeat) treated with radiotherapy in 2005 were estimated at approximately 162,000 and 198,000, respectively. In actual use were 765 linear accelerators, 11 telecobalt machines, 48 GammaKnife machines, 64 ^{60}Co remote-controlled after-loading systems, and 119 ^{192}Ir remote-controlled after-loading systems. The linear accelerator systems used dual-energy function in 498 systems (65%), three-dimensional conformal radiotherapy in 462 (60%), and intensity-modulated radiotherapy in 170 (22%). There were 426 Japanese Society of Therapeutic Radiology and Oncology-certified radiation oncologists, 774 full-time equivalent radiation oncologists, 117 medical physicists, and 1,635 radiation therapists. Geographically, a significant variation was found in the use of radiotherapy, from 0.9 to 2.1 patients/1,000 population. The annual patient load/FTE radiation oncologist was 247, exceeding the Blue Book guidelines level. Patterns of Care Study stratification can clearly discriminate the maturity of structures according to their academic nature and caseload.

Conclusions: The Japanese structure has clearly improved during the past 15 years in terms of equipment and its use, although the shortage of manpower and variations in maturity disclosed by this Patterns of Care Study stratification remain problematic. These constitute the targets for nationwide improvement in quality assurance and quality control. © **2008 Elsevier Inc.**

Structure survey, Radiotherapy facility, Radiotherapy personnel, Radiotherapy equipment, Caseload.

Reprint requests to: Teruki Teshima, M.D., Department of Medical Physics and Engineering, Osaka University Graduate School of Medicine, 1-7 Yamadaoka, Suita, Osaka 565-0871, Japan. Tel: (+81) 6-6879-2570; Fax: (+81) 6-6879-2570; E-mail: teshima@sahs.med.osaka-u.ac.jp

Supported by the Japanese Society of Therapeutic Radiology and Oncology.

Conflict of interest: none.

Acknowledgments—We wish to thank all radiation oncologists and radiation technologists throughout Japan who participated in this survey for their efforts in providing us with information to make this study possible; we also appreciate the continual encouragement and support of Gerald E. Hanks, M.D., former Principal Investigator of Patterns of Care Study, J. Frank Wilson, M.D., current Principal Investigator, and Jean B. Owen, Ph.D., Director, and all other Patterns of Care Study members in the United States and Japan.

Received Oct 10, 2007, and in revised form Dec 12, 2007. Accepted for publication Dec 13, 2007.

INTRODUCTION

The medical care systems of the United States and Japan have very different backgrounds. In 1990, the Patterns of Care Study (PCS) conducted a survey of the 1989 structure of radiation oncology facilities for the entire census of facilities in the United States. The results of the survey, together with trends in the structure of specialization since 1974, were reported in detail by Owen *et al.* (1). In 1991, the Japanese Society of Therapeutic Radiation Oncology (JASTRO) conducted the first national survey of the structure of radiotherapy (RT) facilities in Japan based on their status in 1990, with the results reported by Tsunemoto (2). The first comparison of these two national structure surveys to illustrate the similarities and differences present in 1989–1990 was conducted by Teshima *et al.* (3) and reported in 1995. The resultant international exchange of information proved valuable for both countries, because each could improve their own structure of radiation oncology using those data.

The Japanese structure of radiation oncology has improved in terms of the greater number of cancer patients who are treated with RT, as well as the public awareness of the importance of RT, although problems still exist that should be solved. The JASTRO has conducted national structure surveys every 2 years since 1990 (4). In Japan, an anticancer law was enacted in 2006 in response to patients' urgent petitions to the government. This law strongly advocates the promotion of RT and increasing the number of radiation oncologists (ROs) and medical physicists. The findings of the international comparisons and the consecutive structural data gathered and published by the JASTRO have been useful in convincing the Japanese bureaucracy of the importance of RT. In this report, the recent structure of radiation oncology in Japan is presented, with reference to data obtained from previous international comparisons.

METHODS AND MATERIALS

Between March 2006 and February 2007, the JASTRO conducted a questionnaire using a national structure survey of radiation oncology in 2005. The questionnaire included the number of treatment machines by type, number of personnel by category, and number of patients by type, site, and treatment modality. For variables measured over a period, data were requested for the calendar year 2005. The response rate was 712 (96.9%) of 735 of active facilities. The data from 511 institutions (69.5%) were registered in the International Directory of Radiotherapy Centres in Vienna, Austria in April 2007.

The PCS was introduced in Japan in 1996 (5–11). The PCS in the United States used structural stratification to analyze the national averages for the data in each survey item using two-stage cluster sampling. The Japanese PCS used similar methods. We stratified the RT facilities nationwide into four categories for the regular structure surveys. This stratification was based on academic conditions and the annual number of patients treated with RT in each institution, because the academic institutions require, and have access to, more resources for education and training and the annual caseload also constitutes essential information related to structure. For the present study, the following institutional stratification was used: A1, university hospitals/cancer centers treating ≥440 patients/y; A2, the same type of institutions treating ≤439 patients/y; B1, other national/public hospitals treating ≥130 patients/y; and B2, other national hospital/public hospitals treating ≤129 patients/y.

The Statistical Analysis Systems, version 8.02 (SAS Institute, Cary, NC), software program (12) was used for statistical analyses, and statistical significance was tested using the chi-square test, Student *t* test, or analysis of variance.

RESULTS

Current situation of radiation oncology in Japan

Table 1 shows that the numbers of new patients and total patients (new plus repeat) requiring RT in 2005 were estimated at approximately 162,000 and 198,000, respectively. According to the PCS stratification of institutions, almost 40% of the patients were treated at academic institutions (categories A1 and A2), even though these academic institutions constituted only 18% of the 732 RT facilities nationwide.

The cancer incidence in Japan in 2005 was estimated at 660,578 (13) with approximately 25% of all newly diagnosed patients treated with RT. The number has increased steadily during the past 10 years and is predicted to increase further (4).

Facility and equipment patterns

Table 2 lists the RT equipment and related function. In actual use were 767 linear accelerators, 11 telecobalt machines, 48 Gamma Knife machines, 65 ^{60}Co remote-controlled afterloading systems (RALSs), and 119 ^{192}Ir RALSs. The linear accelerator system used dual-energy function in 498 systems

Table 1. PCS stratification of radiotherapy facilities in Japan

Institution Category	Description	Facilities (*n*)	New patients (*n*)	Average new patients/facility* (*n*)	Total patients (new + repeat) (*n*)	Average total patients/facility* (*n*)
A1	UH and CC (≥440 patients/y)	66	45,866	694.9	54,885	831.6
A2	UH and CC (<440 patients/y)	67	17,161	256.1	21,415	319.6
B1	Other (≥130 patients/y)	290	71,627	247.0	88,757	306.1
B2	Other (<130 patients/y)	289	21,664	75.0	26,116	90.4
Total		712	156,318†	219.5	191,173†	268.5

Abbreviations: PCS = Patterns of Care Study; UH = university hospital; CC = cancer center hospital; Other = other national, city, or public hospital.

* $p < 0.0001$.

† Number of radiotherapy institutions was 735 in 2005, and number of new patients was estimated at approximately 162,000; corresponding number of total patients (new plus repeat) was 198, 000.